Spectral signatures of fractionalization in the frustrated Heisenberg model on the square lattice

Original
Spectral signatures of fractionalization in the frustrated Heisenberg model on the square lattice / Ferrari, F.; Becca, F.. - In: PHYSICAL REVIEW. B. - ISSN 2469-9950. - 98:10(2018), pp. 1-6. [10.1103/PhysRevB.98.100405]

Availability:
This version is available at: 20.500.11767/100035 since: 2019-08-20T15:34:41Z

Publisher:

Published
DOI:10.1103/PhysRevB.98.100405

Spectral signatures of fractionalization in the frustrated Heisenberg model on the square lattice

Francesco Ferrari[1] and Federico Becca[2]

[1]*SISSA-International School for Advanced Studies, Via Bonomea 265, I-34136 Trieste, Italy*
[2]*Democritos National Simulation Center, Istituto Officina dei Materiali del CNR and SISSA-International School for Advanced Studies, Via Bonomea 265, I-34136 Trieste, Italy*

(Dated: September 3, 2018)

We employ a variational Monte Carlo approach to efficiently obtain the dynamical structure factor for the spin-1/2 $J_1 - J_2$ Heisenberg model on the square lattice. Upon increasing the frustrating ratio J_2/J_1, the ground state undergoes a continuous transition from a Néel antiferromagnet to a $\mathbb{Z}_2$ gapless spin liquid. We identify the characteristic spectral features in both phases and highlight the existence of a broad continuum of excitations in the proximity of the spin-liquid phase. The magnon branch, which dominates the spectrum of the unfrustrated Heisenberg model, gradually loses its spectral weight, thus releasing nearly-deconfined spinons, whose signatures are visible even in the magnetically ordered state. Our results provide an important example on how magnons fractionalize into deconfined spinons across a quantum critical point.

Introduction. The existence of fractional excitations is a phenomenon due to the strong interaction between the particles. It refers to the emergence of quasiparticle excitations having quantum numbers that are non-integer multiples of those of the constituent particles (such as electrons) [1]. In two or three spatial dimensions fractionalization is generally associated with emergent gauge fields and can be described in terms of deconfinement of quasiparticles that are free to move, rather than forming bound states. There are several examples of fractionalization, ranging from high-energy physics to condensed matter, where gauge theories show transitions between confining and deconfining phases [2]. One of the most prominent examples is the fractional quantum Hall effect, where the quasiparticles carry fractions of the electron charge [3]. Another important case is given by the spin-charge separation in one-dimensional electronic conductors: here, the electron splits into a *spinon*, which carries spin $S = 1/2$ and no charge, and a *holon*, with $S = 0$ and unit charge e [4, 5]. Also one-dimensional insulators exhibit fractionalization in the spin sector, e.g., the Heisenberg model [6], where elementary excitations are $S = 1/2$ free spinons and not conventional $S = 1$ spin waves [7].

In recent years, motivated by the discovery of high-temperature superconductors, there has been an increasing effort to understand whether spin-charge separation is also possible in two-dimensional Mott insulators. In fact, in two dimensions, magnetic order is likely to develop in the ground state, entailing conventional spin-wave excitations (i.e., $S = 1$ *magnons*) [8]. In this regard, frustrated systems are ideal candidates, since the competition among different super-exchange couplings may prevent the system from developing long-range order [9, 10]. There have been several attempts to obtain fractional excitations in two-dimensional antiferromagnets, ranging from the earliest approaches based upon the resonating-valence bond (RVB) theory [11–13] to alternative theoretical frameworks based on boson-vortex dualities and $\mathbb{Z}_2$ gauge theory [14, 15]. Examples of deconfined excitations have been detected in the Kitaev model [16] or its generalization including Heisenberg terms [17, 18]. Fractionalization has been also invoked to describe continuous phase transitions, where, in contrast to the conventional Landau-Ginzburg-Wilson paradigm, characterized by critical fluctuation of the order parameter, the critical theory contains emergent gauge fields and deconfined quasiparticles with fractional quantum numbers [19, 20]. In this context, dynamical signatures of the fractionalized excitations have been recently considered within a spin model with ring-exchange interactions [21]. Furthermore, the possibility for a coexistence of nearly-free spinons and conventional $S = 1$ magnon excitations has been suggested by recent neutron-scattering experiments on $Cu(DCOO)_2{\cdot}4D_2O$, which have revealed the presence of a very broad spectrum around the wave vector $q = (\pi, 0)$ [and $(0, \pi)$] together with a strong magnon peak around $q = (\pi, \pi)$ [22]. The experimental results were combined with a theoretical analysis based upon variational wave functions and the *unfrustrated* Heisenberg model. However, their theoretical description was not fully satisfactory, since the magnon branch in the whole Brillouin zone was recovered by a variational state that includes magnetic order, while a broad continuum of deconfined excitations was obtained when using a spin-liquid (i.e., RVB) wave function. Still, an intriguing interpretation of these results involves the existence of nearly-deconfined spinons [23], while a more conventional one resorts to magnons with a strong attraction at short length scales [24].

In this paper, we report variational calculations for the frustrated $J_1 - J_2$ spin-1/2 Heisenberg model on the square lattice. Different numerical approaches suggested the existence of a quantum critical point at $J_2/J_1 \approx 0.5$, separating an ordered Néel antiferromagnet and a non-magnetic phase [25–31], whose precise nature is still under debate. By using a recently developed variational technique that can deal with low-energy states with given

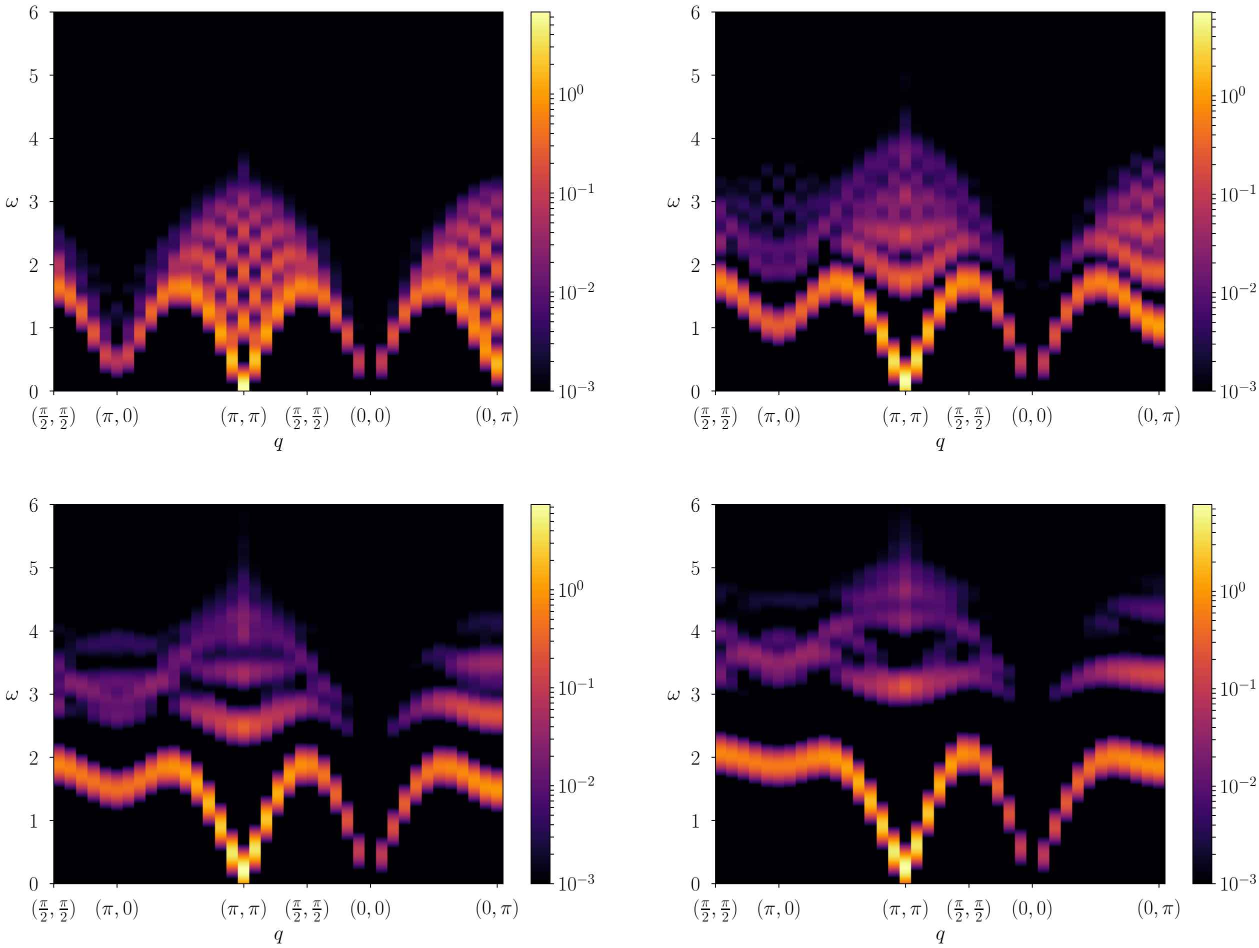

Figure 1: Dynamical spin structure factor of the spatially anisotropic Heisenberg model with $J_2 = 0$. Different values of the inter-chain couplings are reported: $J_1^{\perp}/J_1^{\parallel} = 0.1$ (upper-left), 0.3 (upper-right), 0.5 (lower-left), and 0.7 (lower-right). The square cluster contains $N = 22 \times 22$ sites. Spectral functions have been convoluted with normalized Gaussians with standard deviation $0.1 J_1^{\parallel}$.

momentum q [32, 33], we report the evolution of the dynamical structure factor from the Néel to a gapless $\mathbb{Z}_2$ spin-liquid phase, which is obtained within our approach. The gradual softening and broadening of the spectral signal around $q = (\pi, 0)$ and $(0, \pi)$ when approaching the critical point represents an important hallmark of the spin model. A gapless continuum of free spinons in the spin-liquid phase is ascribed to four Dirac points at $q = (\pm\pi/2, \pm\pi/2)$. Moreover, our results suggest the possibility that nearly-deconfined spinons already exist within the Néel phase close to the critical point. This work provides the evidence that the dynamical signatures of fractionalization observed for the sign-free model of Ref. [21] is a generic feature of continuous quantum phase transitions in frustrated spin models.

Model and method. We consider the $J_1 - J_2$ Heisenberg model on the square lattice with $N = L \times L$ sites:

$$\mathcal{H} = J_1^{\parallel} \sum_i \mathbf{S}_i \cdot \mathbf{S}_{i+y} + J_1^{\perp} \sum_i \mathbf{S}_i \cdot \mathbf{S}_{i+x} + J_2 \sum_i \left(\mathbf{S}_i \cdot \mathbf{S}_{i+x+y} + \mathbf{S}_i \cdot \mathbf{S}_{i+x-y}\right), \tag{1}$$

where $\mathbf{S}_i = (S_i^x, S_i^y, S_i^z)$ is the spin-1/2 operator on the site i; the Hamiltonian contains both nearest-neighbor terms along x and y spatial directions ($J_1^{\perp}$ and $J_1^{\parallel}$, respectively) and next-nearest-neighbor ones along $x+y$ and $x-y$ (J_2). Here, we consider $J_1^{\perp} \neq J_1^{\parallel}$ only when $J_2 = 0$, while we take $J_1^{\perp} = J_1^{\parallel} = J_1$ when $J_2 > 0$. The central aim of this work is to assess the dynamical structure factor at zero temperature, defined by:

$$S^a(q,\omega) = \sum_\alpha |\langle \Upsilon_\alpha^q | S_q^a | \Upsilon_0 \rangle|^2 \delta(\omega - E_\alpha^q + E_0), \tag{2}$$

where $|\Upsilon_0\rangle$ is the ground state of the system with energy

E_0, $\{|\Upsilon_\alpha^q\rangle\}$ are the excited states with momentum q (relative to the ground state) and energy E_α^q, and S_q^a is the Fourier transform of the spin operator S_i^a.

For generic values of the frustrating ratio J_2/J_1, there are no exact methods that allow us to evaluate the dynamical structure factor. Therefore, we resort to considering a suitable approximation, by employing Gutzwiller projected fermionic wave functions to construct accurate variational states to describe both the ground state and low-energy excitations. In particular, we consider an auxiliary superconducting (BCS) Hamiltonian:

$$\mathcal{H}_0 = \sum_{i,j,\sigma} t_{i,j} c_{i,\sigma}^\dagger c_{j,\sigma} + \sum_{i,j} \Delta_{i,j} c_{i,\uparrow}^\dagger c_{j,\downarrow}^\dagger + h.c. + \Delta_{\mathrm{AF}} \sum_i e^{iQR_i} \left(c_{i,\uparrow}^\dagger c_{i,\downarrow} + c_{i,\downarrow}^\dagger c_{i,\uparrow} \right), \quad (3)$$

where, $c_{i,\sigma}^\dagger$ ($c_{i,\sigma}$) creates (destroys) an electron with spin $\sigma = \pm 1/2$ on the site i; $t_{i,j}$ is a complex nearest-neighbor hopping generating a staggered magnetic flux on elementary (square) plaquettes [12] (when $J_1^\perp \neq J_1^\parallel$, different amplitudes along x and y are considered); $\Delta_{i,j} = \Delta_{j,i}$ is a real singlet pairing with d_{xy} symmetry [34]; finally, Δ_{AF} is an antiferromagnetic parameter pointing along x, with periodicity given by the pitch vector $Q = (\pi, \pi)$. A suitable variational wave function for the spin system is obtained by taking the ground state $|\Phi_0\rangle$ of the auxiliary Hamiltonian $\mathcal{H}_0$ and projecting out all the configurations with at least one empty or doubly occupied site:

$$|\Psi_0\rangle = \mathcal{P}_{S_z} \mathcal{J}_s \mathcal{P}_G |\Phi_0\rangle, \quad (4)$$

where $\mathcal{P}_G = \prod_i (n_{i,\uparrow} - n_{i,\downarrow})^2$ ($n_{i,\sigma} = c_{i,\sigma}^\dagger c_{i,\sigma}$ being the local electron density per spin σ on site i) is the Gutzwiller projector. In addition, the spin-spin Jastrow factor $\mathcal{J}_s = \exp\left(1/2 \sum_{i,j} v_{i,j} S_i^z S_j^z\right)$ is also considered to include relevant spin-wave fluctuations over the staggered magnetization induced by Δ_{AF} [35]. Finally, $\mathcal{P}_{S_z}$ is the projection onto the subspace with $S_{\mathrm{tot}}^z = \sum_i S_i^z = 0$. Due to the correlated nature of the variational wave function, the evaluation of all physical quantities requires a Monte Carlo sampling. All the parameters inside $\mathcal{H}_0$, as well as the Jastrow pseudo-potential $v_{i,j}$ (which is taken to be translationally invariant), are optimized by mean of the stochastic reconfiguration technique, to minimize the variational energy of $|\Psi_0\rangle$ [36].

Following Refs. [22, 32, 33], for each momentum q, we define a (non-orthogonal) set of states, labeled by the site position R, which can be used to approximate the exact low-energy excitations:

$$|q, R\rangle = \mathcal{P}_{S_z} \mathcal{J}_s \mathcal{P}_G \frac{1}{\sqrt{N}} \sum_i e^{iqR_i} \sum_\sigma \sigma c_{i+R,\sigma}^\dagger c_{i,\sigma} |\Phi_0\rangle. \quad (5)$$

By diagonalizing the Heisenberg Hamiltonian within the subspace $\{|q, R\rangle\}$, a set of approximate excited states $|\Psi_n^q\rangle = \sum_R A_R^{n,q} |q, R\rangle$, with energies $\{E_n^q\}$, can be constructed, as described in Ref. [33]. Then, the dynamical structure factor of Eq. (2) is given by:

$$S^a(q, \omega) = \sum_n |\langle \Psi_n^q | S_q^a | \Psi_0 \rangle|^2 \delta(\omega - E_n^q + E_0^{\mathrm{var}}), \quad (6)$$

where E_0^{var} is the variational energy of $|\Psi_0\rangle$. We emphasize that, within this variational approximation, the sum over excited states runs over at most N states (instead of an exponentially large number of the exact formulation). Our approach is particularly suited to capture two-spinon excitations, both when they form a bound state (for example, a magnon) and when they remain free. In the following, we consider the z-component (i.e., $a \equiv z$) of the dynamical structure factor of Eq. (6). When Δ_{AF} is finite in the auxiliary Hamiltonian of Eq. (3), the variational state breaks spin $SU(2)$ symmetry and $S^z(q, \omega)$ probes *transverse* fluctuations; instead, for the spin-liquid wave function, with $\Delta_{\mathrm{AF}} = 0$, all the components of the dynamical structure factor give the same contribution. We want to stress the important fact that all the quantities that define the dynamical structure factor of Eq. (6) can be computed within a variational Monte Carlo scheme (*without* any sign problem and *without* any analytic continuation).

Before Gutzwiller projection, the excited states are particle-hole excitations in the BCS spectrum, which we identify as two-spinon terms. We expect this approach to be suited to describe excited states of deconfined phases, as for example in one-dimensional spin models [33]. Nonetheless, bound states of two spinons can be also obtained, such as single-magnon excitations [22]. The possibility to capture the multi-magnon features is more problematic. Indeed, for the unfrustrated Heisenberg model, our calculations (as well as the ones of Ref. [22]) show that the multi-magnon continuum in the

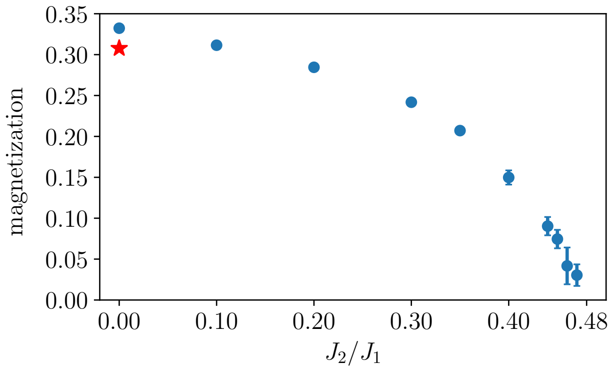

Figure 2: Variational results for the ground-state magnetization of the $J_1 - J_2$ Heisenberg model. The results are obtained in the thermodynamic limit, by extrapolating the isotropic spin-spin correlations at the maximum distance in the $L \times L$ clusters with L ranging from 10 to 22. The exact result for the unfrustrated Heisenberg model, obtained by quantum Monte Carlo [40, 41], is also reported for comparison (red star).

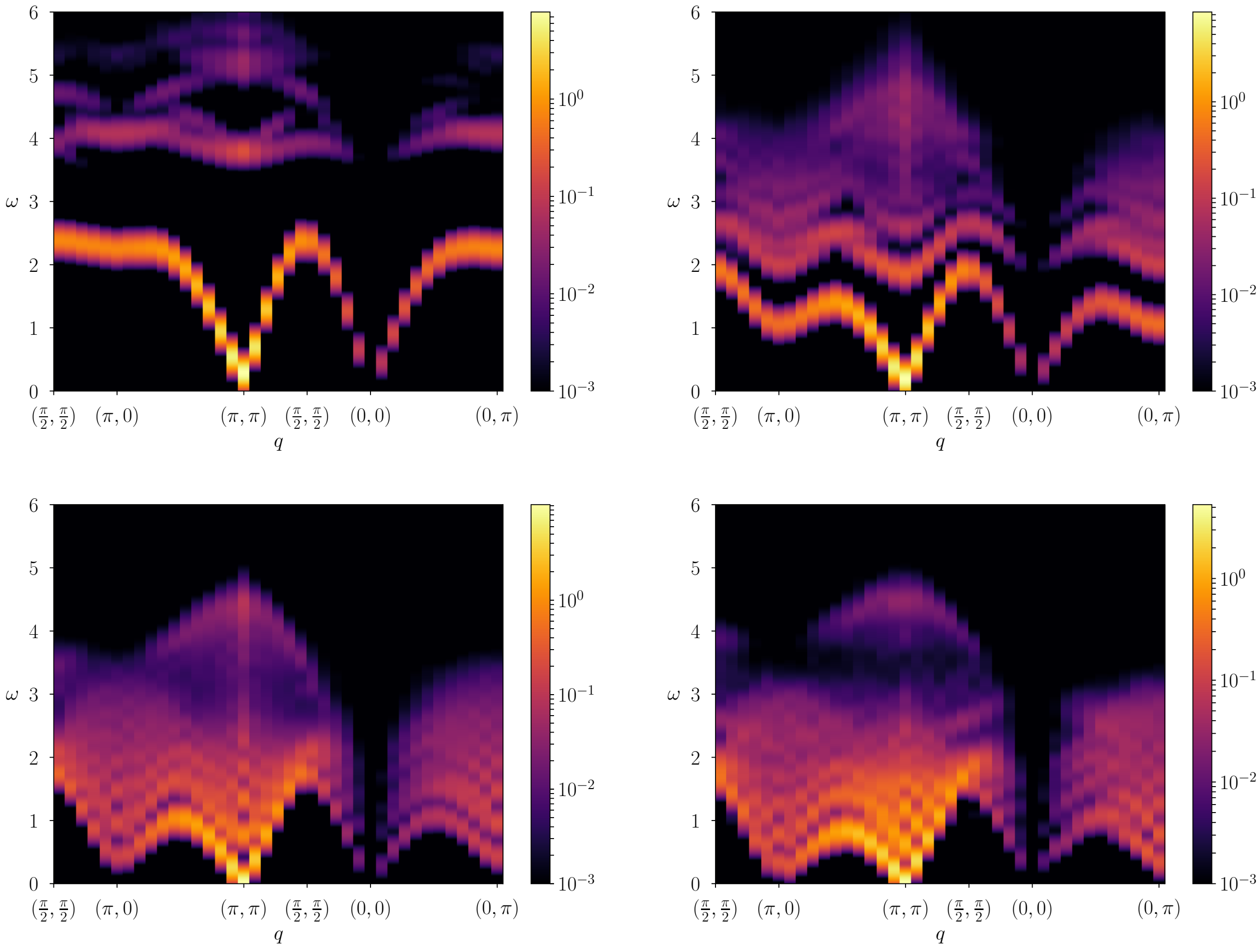

Figure 3: Dynamical spin structure factor of the $J_1 - J_2$ Heisenberg model. Different values of the frustrating ratio are reported: $J_2/J_1 = 0$ (upper-left), 0.3 (upper-right), 0.45 (lower-left), and 0.55 (lower-right). The antiferromagnetic parameter $\Delta_{\rm AF}$ is finite in the first three cases, while it is vanishing for the last one. The square cluster contains $N = 22 \times 22$ sites. Spectral functions have been convoluted with normalized Gaussians with standard deviation $0.1J_1$.

transverse signal is very weak and, most probably, cannot account for the actual results [37].

Results. We start from the nearest-neighbor Heisenberg model with $J_1^\perp \neq J_1^\parallel$ and $J_2 = 0$. For $J_1^\perp = 0$, the lattice is decoupled into L copies of a one-dimensional chain with L sites. In this case, there is no magnetic long-range order and the elementary excitations are spinons, which form a continuum of excitations in the dynamical structure factor [38]. The variational Monte Carlo procedure described above gives an excellent description of the exact spectrum [33]. As soon as $J_1^\perp$ is turned on, the ground state develops Néel magnetic order and a coherent magnon excitation settles down at low energies [39]. Within our variational approach, the optimal antiferromagnetic parameter $\Delta_{\rm AF}$ is finite as soon as $J_1^\perp > 0$ (in this case, no pairing terms are considered). Our calculations show that the spinon excitations, which characterize the spectrum of the one-dimensional Heisenberg model, are gradually pushed to a narrow region at higher energies, progressively losing their spectral weight. Concurrently, at low energies, a strong magnon branch sets in. The results for different values of the inter-chain super-exchange $J_1^\perp$ are shown in Fig. 1. For $J_1^\perp/J_1^\parallel = 0.1$, the dynamical structure factor still resembles the one of a pure Heisenberg chain [33]. However, at variance with $J_1^\perp = 0$, where the spectrum does not depend upon q_x, here there is already a sensible difference in the intensity of the lowest-energy excitations for different q_x: for example, at $q_y = \pi$, the strongest signal is found at $q_x = \pi$, due to the presence of the (weak) Néel order. As $J_1^\perp/J_1^\parallel$ is raised, the gap at $(\pi, 0)$ and $(0, \pi)$ increases. In addition, the former one gains spectral weight, while the latter one loses it, until the limit of $J_1^\perp/J_1^\parallel = 1$ is reached, where the rotational symmetry of the square lattice is recovered and the two momenta become equivalent. Remarkably, the broad continuum that characterizes the quasi-one-dimensional spectrum gradually disappears when approaching the two-dimensional limit. Here, the multi-magnon continuum is very weak, especially at low energies. In this sense, it would be tantalizing to discriminate between two possible channels for the magnon decay, one driven by a magnon-magnon interaction, leading to a multi-magnon decay, and another one in which the magnon splits into two spinons. While the latter one can be captured by the variational *Ansatz* of Eq. (5), the former one may go beyond our description.

The indication that deconfined spinons are released when approaching a quantum critical point comes from the analysis of the more interesting case with $J_1^\perp = J_1^\parallel$ and frustrating J_2. First of all, to locate the quantum phase transition from the Néel to the magnetically disordered phase, we compute the staggered magnetization using the isotropic spin-spin correlation at maximum distance for different lattice size, and we extrapolate to the thermodynamic limit. The results are reported in Fig. 2 and show that the magnetization drops to zero at $J_2/J_1 \approx 0.48$, as suggested by recent variational calculations on the spin gap [26] (the exact result for the unfrustrated Heisenberg model, obtained by quantum Monte Carlo [40, 41], is also reported for comparison). The disappearance of the order parameter is related to the fact that $\Delta_{\rm AF} \to 0$ in the auxiliary Hamiltonian (3). In the region where $\Delta_{\rm AF} = 0$, a finite paring amplitude with d_{xy} symmetry can be stabilized, but no energy gain is obtained by allowing translational symmetry breaking in hopping or pairing terms, thus implying that no valence-bond order is present. A comparison with exact results on the 6×6 lattice provides the degree of accuracy of our approach for both the unfrustrated and the highly-frustated cases [42]. Then, the results on the 22×22 cluster for different values of J_2/J_1 are reported in Fig. 3. For weak frustration, the magnon branch is well defined in the entire Brillouin zone, including $q = (\pi, 0)$, and the multi-magnon continuum is very weak. In the unfrustrated limit with $J_2 = 0$, we recover the well-known result that the lowest-energy excitation at $q = (\pi, 0)$ [and $q = (0, \pi)$] is slightly lower than the one at $q = (\pm\pi/2, \pm\pi/2)$ [22, 23]. However, our variational approach is not able to capture the asymmetry between the weights of the magnon pole for these momenta. Still within the ordered phase, two principal effects are visible when increasing J_2/J_1. The first one is a gradual broadening of the spectrum, with the formation of a wide continuum close to the magnon branch. The second one is a clear reduction of the lowest-energy excitation at $q = (\pi, 0)$, as already suggested in Ref. [26]. This fact is related to the structure of the BCS spectrum of the auxiliary Hamiltonian (before Gutzwiller projection), which contains staggered fluxes and a finite d_{xy} pairing. Here, there are four Dirac points at $q = (\pm\pi/2, \pm\pi/2)$, leading to two-spinon excitations that are gapless, not only for $q = (0, 0)$, (π, π), but also at $(\pi, 0)$ and $(0, \pi)$. The above choice of the parameters (giving the best variational energy) corresponds to a gapless $\mathbb{Z}_2$ spin liquid, dubbed Z2Azz13 in Ref. [43]. In presence of the Gutzwiller projection the spectrum is clearly gapless at (π, π), while the gap at $(\pi, 0)$ and $(0, \pi)$ may possess much larger size effects [42]. A similar situation appeared within the single-mode approximation of Ref. [26], where a variance extrapolation was necessary to prove the existence of gapless excitations at $(\pi, 0)$ and $(0, \pi)$. Within the antiferromagnetic region, the presence of a broad continuum, which can be captured by our variational *Ansatz* with two-spinon excitations, suggests that nearly-deconfined spinons may be present even in the ordered phase [23], as evoked few years ago by field-theory arguments [14]. Yet, in the $J_1 - J_2$ model, fully deconfined spinon excitations are actually present beyond the critical point, for $0.48 \lesssim J_2/J_1 \lesssim 0.6$.

Conclusions. In this work, we assessed the dynamical properties of a highly-frustrated (non-integrable) spin system, by using a variational Monte Carlo approach based upon a restricted basis set of approximate excited states [32]. When increasing frustration, a gradual broadening of the spectrum takes place in the whole Brillouin zone, suggesting that no coherent magnon excitations exist at the transition point [19, 20]. A second important outcome is the development of gapless modes at $q = (\pi, 0)$ and $q = (0, \pi)$, which also characterize the spin-liquid phase found for $0.48 \lesssim J_2/J_1 \lesssim 0.6$. At variance with the unfrustrated model studied in Ref. [21], where these gapless excitations are due to an emergent $O(4)$ symmetry (involving both Néel and valence-bond-solid order parameters), here they originate from the four Dirac points at $q = (\pm\pi/2, \pm\pi/2)$ in the spinon spectrum of the $\mathbb{Z}_2$ spin liquid. Finally, for weak frustrations, the concomitant existence of a magnon pole along with the broad continuum captured by two-spinon excitations hints the possibility to have an unconventional antiferromagnetic state, where magnons and nearly-deconfined spinons coexist [22, 23].

Acknowledgements. We thank A. Parola and S. Sorella for important suggestions and fruitful conversations. We also acknowledge A. Sandvik, H. Shao, and R. Verresen for sharing their results on the Heisenberg model with us and A. Chernyshev for useful discussions.

Note added. During the completion of this paper, we became aware of a similar work, based upon semi-analytical techniques, which also studied spectral properties of the frustrated Heisenberg model, supporting the possibility for a deconfined criticality when increasing J_2/J_1 [44].

[1] See for example, R.B. Laughlin, Rev. Mod. Phys. **71**, 863 (1999).
[2] J.B. Kogut, Rev. Mod. Phys. **51**, 659 (1979).
[3] R.B. Laughlin, Phys. Rev. Lett. **50**, 1395 (1983).

[4] J.M. Luttinger, J. Math. Phys. **4**, 1154 (1963).
[5] F.D.M. Haldane, J. Phys. C: Solid State Phys. **14**, 2585 (1981).
[6] H. Bethe, Z. Phys. **71**, 205 (1931).
[7] L.D.Faddeev and L.A.Takhtajan, Phys. Lett. A **85**, 375 (1981).
[8] P.W. Anderson, Phys. Rev. **86**, 694 (1952).
[9] C. Lacroix, P. Mendels, and F. Mila, Introduction to Frustrated Magnetism (Springer, 2011).
[10] L. Savary and L. Balents, Rep. Prog. Phys. **80**, 016502 (2017).
[11] G. Baskaran and P.W. Anderson, Phys. Rev. B **37**, 580 (1988).
[12] I. Affleck and J.B. Marston, Phys. Rev. B **37**, 3774 (1988).
[13] N. Read and S. Sachdev, Phys. Rev. Lett. **66**, 1773 (1991).
[14] L. Balents, M.P.A. Fisher, and C. Nayak, Phys. Rev. B **60**, 1654 (1999).
[15] T. Senthil and M.P.A. Fisher, Phys. Rev. B **62**, 7850 (2000).
[16] A. Yu. Kitaev, Ann. Phys. (Amsterdam) **321**, 2 (2006).
[17] J. Knolle, D.L. Kovrizhin, J.T. Chalker, and R. Moessner, Phys. Rev. Lett. **112**, 207203 (2014).
[18] M. Gohlke, R. Verresen, R. Moessner, and F. Pollmann, Phys. Rev. Lett. **119**, 157203 (2017).
[19] T. Senthil, A. Vishwanath, L. Balents, S. Sachdev, M.P.A. Fisher, Science **303**, 1490 (2004).
[20] T. Senthil, L. Balents, S. Sachdev, A. Vishwanath, M.P.A. Fisher, Phys. Rev. B **70**, 144407 (2004).
[21] N. Ma, G.-Y. Sun, Y.-Z. You, C. Xu, A. Vishwanath, A.W. Sandvik, and Z.-Y. Meng, arXiv:1803.01180
[22] B. Dalla Piazza, M. Mourigal, N.B. Christensen, G.J. Nilsen, P. Tregenna-Piggott, T.G. Perring, M. Enderle, D.F. McMorrow, D.A. Ivanov, and H.M. Rønnow, Nat. Phys. **11**, 62 (2015).
[23] H. Shao, Y.-Q. Qin, S. Capponi, S. Chesi, Z.-Y. Meng, and A.W. Sandvik, Phys. Rev. X **7** 041072 (2017).
[24] M. Powalski, K.P. Schmidt, and G.S. Uhrig, SciPost Phys. **4**, 001 (2018).
[25] H.-C. Jiang, H. Yao, and L. Balents, Phys. Rev. B **86**, 024424 (2012).
[26] W.-J. Hu, F. Becca, A. Parola, and S. Sorella, Phys. Rev. B **88**, 060402 (2013).
[27] S.-S. Gong, W. Zhu, D.N. Sheng, O.I. Motrunich, and M.P.A. Fisher, Phys. Rev. Lett. **113**, 027201 (2014).
[28] L. Wang, Z.-C. Gu, F. Verstraete, and X.-G. Wen, Phys. Rev. B **94**, 075143 (2016).
[29] D. Poilblanc and M. Mambrini, Phys. Rev. B **96**, 014414 (2017).
[30] L. Wang and A.W. Sandvik, arXiv:1702.08197.
[31] R. Haghshenas and D.N. Sheng, Phys. Rev. B **97**, 174408 (2018).
[32] T. Li and F. Yang, Phys. Rev. B **81**, 214509 (2010).
[33] F. Ferrari, A. Parola, S. Sorella, and F. Becca, Phys. Rev. B **97**, 235103 (2018).
[34] The most natural choice is to take a d_{xy} pairing on the second-neighbor bonds of the lattice. However, in order to have gapless (Dirac) points located at the commensurate momenta $q = (\pm\frac{\pi}{2}, \pm\frac{\pi}{2})$ and achieve a better accuracy, we consider a pairing with d_{xy} symmetry at the fifth-neighbor distance.
[35] E. Manousakis, Rev. Mod. Phys. **63**, 1 (1991).
[36] S. Sorella, Phys. Rev. B **71**, 241103(R) (2005).
[37] A.W. Sandvik and R.R.P. Singh, Phys. Rev. Lett. **86**, 528 (2001).
[38] J.-S. Caux and R. Hagemans, J. Stat. Mech. (2006) P12013.
[39] I. Affleck, M.P. Gelfand, and R.R.P. Singh, J. Phys. A: Math. Gen. **27**, 7313 (1994).
[40] M. Calandra Buonaura and S. Sorella, Phys. Rev. B **57**, 11446 (1998).
[41] A.W. Sandvik, Phys. Rev. B **56**, 11678 (1997).
[42] See Supplemental Material.
[43] X.-G. Wen, Phys. Rev. B **65**, 165113 (2002).
[44] S.-L. Yu, W. Wang, Z.-Y. Dong, Z.-J. Yao, J.-X. Li, arXiv:1805.07915.